

# **SANDIA REPORT**

SAND2015-8598

Unlimited Release

Printed October 2015

## **Estimating Parameters for the PVsyst Version 6 Photovoltaic Module Performance Model**

Clifford Hansen

Prepared by  
Sandia National Laboratories  
Albuquerque, New Mexico 87185 and Livermore, California 94550

Sandia National Laboratories is a multi-program laboratory managed and operated by Sandia Corporation, a wholly owned subsidiary of Lockheed Martin Corporation, for the U.S. Department of Energy's National Nuclear Security Administration under contract DE-AC04-94AL85000.

Approved for public release; further dissemination unlimited.



**Sandia National Laboratories**

Issued by Sandia National Laboratories, operated for the United States Department of Energy by Sandia Corporation.

**NOTICE:** This report was prepared as an account of work sponsored by an agency of the United States Government. Neither the United States Government, nor any agency thereof, nor any of their employees, nor any of their contractors, subcontractors, or their employees, make any warranty, express or implied, or assume any legal liability or responsibility for the accuracy, completeness, or usefulness of any information, apparatus, product, or process disclosed, or represent that its use would not infringe privately owned rights. Reference herein to any specific commercial product, process, or service by trade name, trademark, manufacturer, or otherwise, does not necessarily constitute or imply its endorsement, recommendation, or favoring by the United States Government, any agency thereof, or any of their contractors or subcontractors. The views and opinions expressed herein do not necessarily state or reflect those of the United States Government, any agency thereof, or any of their contractors.

Printed in the United States of America. This report has been reproduced directly from the best available copy.

Available to DOE and DOE contractors from

U.S. Department of Energy  
Office of Scientific and Technical Information  
P.O. Box 62  
Oak Ridge, TN 37831

Telephone: (865) 576-8401  
Facsimile: (865) 576-5728  
E-Mail: [reports@adonis.osti.gov](mailto:reports@adonis.osti.gov)  
Online ordering: <http://www.osti.gov/bridge>

Available to the public from

U.S. Department of Commerce  
National Technical Information Service  
5285 Port Royal Rd.  
Springfield, VA 22161

Telephone: (800) 553-6847  
Facsimile: (703) 605-6900  
E-Mail: [orders@ntis.fedworld.gov](mailto:orders@ntis.fedworld.gov)  
Online order: <http://www.ntis.gov/help/ordermethods.asp?loc=7-4-0#online>



# Estimating Parameters for the PVsyst Version 6 Photovoltaic Module Performance Model

Clifford Hansen  
Photovoltaic and Distributed Systems Department, Sandia National Laboratories  
P.O. Box 5800  
Albuquerque, New Mexico 87185-1033

## Abstract

We present an algorithm to determine parameters for the photovoltaic module performance model encoded in the software package PVsyst™ version 6. Our method operates on current-voltage (I-V) measured over a range of irradiance and temperature conditions. We describe the method and illustrate its steps using data for a 36 cell crystalline silicon module. We qualitatively compare our method with one other technique for estimating parameters for the PVsyst™ version 6 model.

## **ACKNOWLEDGMENTS**

# CONTENTS

1. Introduction.....	9
2. PVsyst Module Performance Model.....	11
3. Methodology .....	13
3.1. Data.....	13
3.2. Parameter Estimation Method.....	14
Step 1: Temperature coefficients.....	14
Step 2: Determine diode factor terms.....	15
Step 3: Determine parameters for each I-V curve.....	19
Step 4: Obtain parameter values for the PVsyst single diode model .....	22
3. Qualitative Comparison with Other Methods.....	27
4. References.....	29
Distribution .....	30

## FIGURES

Figure 1. Parameter Estimation method.....	14
Figure 2. Determination of $\alpha_{Isc}$ . ....	15
Figure 3. Examples of measured I-V curves for which $R_{SH} < 0$ .....	17
Figure 4. Estimation of diode factor parameters.....	19
Figure 5. Error (percent) in performance parameters for fitted I-V curves. ....	22
Figure 6. Determination of $I_{L0}$ . ....	23
Figure 7. Determination of $I_{00}$ and $\epsilon_G$ .....	24
Figure 8. Determination of parameters for $R_{SH}$ . ....	25
Figure 9. Determination of $R_{S0}$ . ....	26

## TABLES

Table 1. Parameters for example module. ....	26
--	----

## NOMENCLATURE

CDF	cumulative distribution function
DHI	diffuse horizontal irradiance
DOE	Department of Energy
DNI	direct normal irradiance
GHI	global horizontal irradiance
GUM	Guide to the Expression of Uncertainty in Measurement
NREL	National Renewable Energy Laboratory
POA	plane-of-array
PV	photovoltaic
SNL	Sandia National Laboratories



# 1. INTRODUCTION

The popular PVsyst™ software [1], [2] for modeling photovoltaic system performance employs a single diode model (e.g., [3]) to compute the I-V curve for a module or string of modules at given irradiance and temperature conditions. A single diode model requires a number of parameters to be estimated, preferably from measured I-V curves. Many available parameter estimation methods use only short circuit, open circuit and maximum power points for a single I-V curve at standard test conditions together with temperature coefficients determined from testing of individual cells. In contrast, module testing frequently records I-V curves over a wide range of irradiance and temperature conditions, such as those specified in IEC 61853-1 [4], which, when available, should also be used to parameterize the performance model.

Parameter estimation for single diode models has been challenging due to the model's use of an implicit equation describing the relationship between current and voltage. In earlier work [5] we present an estimation method that avoids several commonly-used simplifying approximations and makes use of a full range of I-V curves and demonstrate the method using the photovoltaic module performance model in [De soto]. In this work, we adapt the techniques in [Hansen] to present an algorithm to determine parameters for the photovoltaic module performance model encoded in PVsyst™ version 6.

In Section 2, we present the single diode model implemented in PVsyst™ Version 6 We present our parameter estimation method in Section 3. In Section 4 we compare our method with the method published by Sauer et al. [6], [7].

The parameter estimation method described here-in is the subject of U.S. Provisional Patent Application Number 62/134,413, filed March 17, 2015, entitled "Methods for Estimating Photovoltaic Module Performance Model Parameters."



## 2. PVSYST MODULE PERFORMANCE MODEL

The single diode model encoded in the PVsyst™ Version 6 software predicts module current  $I$  and voltage  $V$  as a function of module-averaged cell temperature  $T_C$  and effective irradiance  $E$ . Effective irradiance ( $\text{W/m}^2$ ) is the irradiance reaching a module's cells that corresponds to the electrical current generated by the cells. Effective irradiance differs from broadband plane-of-array irradiance due to:

- Reflection, scattering and/or absorption of irradiance by the module's materials or soiling on the module's face;
- The spectral response of the cells.

Effective irradiance can be directly measured with a spectrally-matched reference cell co-planar with the module, or modeled from plane-of-array irradiance measured with a broadband instrument. Uncertainty in predictions of module output can be reduced by use of measured effective irradiance [8]. When effective irradiance is modeled, the accuracy of the model can significantly affect the accuracy of module output predictions [9]. Here, we assume that appropriate effective irradiance data are available.

The module performance model in the PVsyst™ Version 6 software is described in [2], [7], and comprises the single diode equation

$$I = I_L - I_O \left[ \exp\left(\frac{V + IR_S}{\gamma V_{th}}\right) - 1 \right] - \frac{V + IR_S}{R_{SH}} \quad (1)$$

together with the following auxiliary equations

$$I_L = I_L(E, T_C) = \frac{E}{E_0} [I_{L0} + \alpha_{Isc}(T_C - T_0)] \quad (2)$$

$$I_O = I_O(T_C) = I_{O0} \left[ \frac{T_C}{T_0} \right]^3 \exp\left[ \frac{q\mathcal{E}_G}{k\gamma} \left( \frac{1}{T_0} - \frac{1}{T_C} \right) \right] \quad (3)$$

$$\gamma = \gamma_0 + \mu_\gamma (T_C - T_0) \quad (4)$$

$$R_{SH} = R_{SH,base} + (R_{SH,0} - R_{SH,base}) \exp\left(-R_{SH,exp} \frac{E}{E_0}\right) \quad (5)$$

$$R_{SH,base} = \max\left[ \frac{R_{SH,ref} - R_{SH,0} \exp(-R_{shexp})}{1 - \exp(-R_{shexp})}, 0 \right] \quad (6)$$

$$R_S = R_{S0} \quad (7)$$

In Eq. (1)

- $I_L$  is the photo-generated current (A),
- $I_O$  is the dark saturation current (A),
- $\gamma$  is the diode ideality factor (unitless),

$V_{th} = N_s k T_C / q$  is termed the thermal voltage (V) for the module, which is determined from cell temperature  $T_C$  (K), Boltzmann's constant  $k$  (J/K) and the elementary charge  $q$  (coulomb),

- $k$  is Boltzmann's constant ( $1.38066 \times 10^{-23}$  J/K),
- $q$  is the elementary charge ( $1.60218 \times 10^{-19}$  coulomb),
- $R_s$  is the series resistance ( $\Omega$ ),
- $R_{SH}$  is the shunt resistance ( $\Omega$ ).

The quantities  $I_L$ ,  $I_0$ ,  $\gamma$ ,  $R_s$  and  $R_{SH}$  are frequently termed the 'five parameters' although more precisely these quantities should be described as variables, as they depend on the exogenous quantities  $T_C$  and  $E$ . By contrast, a parameter is a fixed quantity that is endogenous to the model.

In Eq. (2) through (7) the subscript  $\sim_0$  indicates a value at the reference conditions  $E_0$  and  $T_0$  for effective irradiance and cell temperature, respectively; typical values are  $E_0 = 1000$  W/m<sup>2</sup> and  $T_0 = 298$ K. Other parameters appearing in Eq. (2) through (7):

- $\alpha_{I_{sc}}$  is the temperature coefficient for  $I_{sc}$  (A/K),
- $\varepsilon_G$  is the effective band gap (eV),
- $\mu_\gamma$  is the temperature coefficient for the diode ideality factor (1/K),
- $R_{SH,0}$  is the shunt resistance in the absence of irradiance ( $\Omega$ ),
- $R_{SH,ref}$  is the shunt resistance at reference irradiance  $E_0$  ( $\Omega$ ),
- $R_{SHexp}$  is an empirical term describing the change of shunt resistance with irradiance (unitless).

The parameters to be estimated are:  $\alpha_{I_{sc}}$ ,  $I_{L0}$ ,  $I_{O0}$ ,  $\varepsilon_G$ ,  $\gamma_0$ ,  $\mu_\gamma$ ,  $R_{SH,0}$ ,  $R_{SH,ref}$ ,  $R_{SHexp}$  and  $R_{S0}$ . We note that here, we estimate an effective band gap  $\varepsilon_G$  rather than imposing a theoretical value for the semiconductor material. Parameter estimation proceeds as indicated in Figure 1 beginning with measurement of a set of I-V curves over a range of irradiance and cell temperature conditions. Next, values are determined for each I-V curve for the five parameters in the single diode equation (Eq. (1)). Finally, parameter values are determined for the auxiliary equations that complete the single diode model. Step 3 of the method presented here is in common with the method that is described in [5] for the single diode model in [10].

### 3. METHODOLOGY

We describe the data needed for parameter estimation and outline the estimation method.

#### 3.1. Data

Data required for parameter estimation fall into two categories: data for determining temperature coefficients; and data for estimating all other model parameters.

For determination of temperature coefficients we assume that I-V curves are measured either outdoors with air mass near 1.5 and angle of incidence zero, or indoors using a flash tester calibrated to these conditions. Concurrent with I-V curves, average cell temperature  $T_c$  should be measured or estimated and plane-of-array (POA) irradiance should be measured. Cell temperature is frequently estimated from measurements of module back-surface temperature. For temperature coefficient determination plane-of-array (POA) irradiance should be maintained near  $1000 \text{ W/m}^2$  while module temperature is varied; generally a range of  $25^\circ\text{C}$  is sufficient. POA irradiance preferably comprises effective irradiance  $E$ , measured using a matched reference cell, but for determining temperature coefficients it is acceptable to use instead broadband POA irradiance  $G_{POA}$  measured with a pyranometer.

For estimating all other model parameters we assume that I-V curves are measured either outdoors or indoors over wide ranges of cell temperatures and effective irradiance, which are also measured concurrent with each I-V curve. If POA irradiance is measured with a broadband instrument it must be adjusted to effective irradiance by application of appropriate reflection, soiling and spectral adjustments.

We illustrate the parameter estimation process using measured I-V curves for a 36-cell Mitsubishi PV-UE125MF5N 125W crystalline silicon module. I-V curves for temperature coefficients and for all other model parameters were measured during outdoor testing in Albuquerque, NM. In these data cell temperature is estimated from the average of three thermocouples attached to the module's backsheet. Effective irradiance is measured in the module's POA with a silicon reference cell.

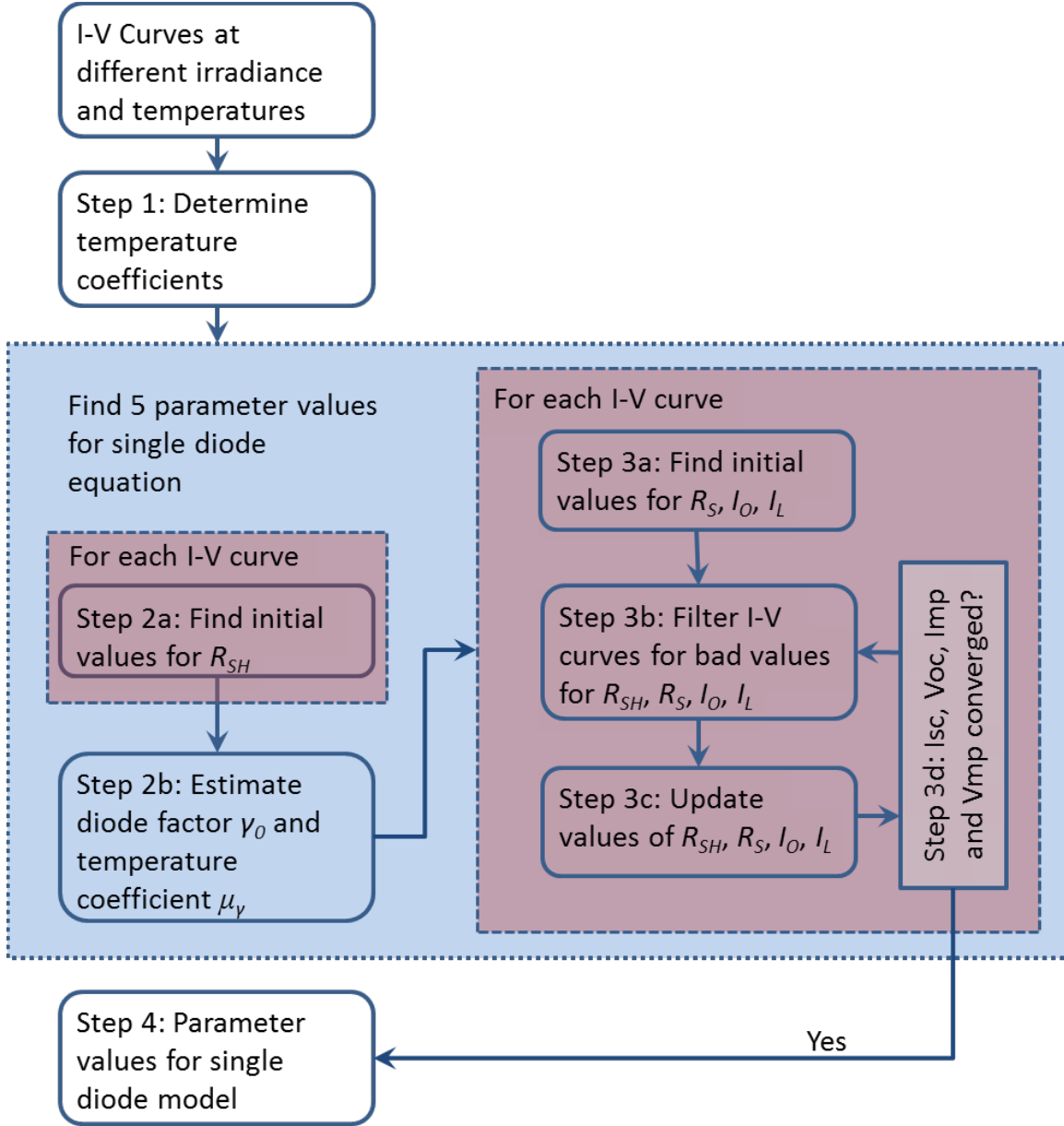


Figure 1. Parameter Estimation method.

### 3.2. Parameter Estimation Method

#### Step 1: Temperature coefficients

We assume a linear device and express the change in  $I_{SC}$  with temperature as

$$I_{SC} = \frac{E}{E_0} \left( I_{SC0} + \alpha_{I_{sc}} (T_C - T_0) \right) \quad (8)$$

where  $I_{SC0}$  and  $\alpha_{I_{sc}}$  are unknown terms. We re-arrange to obtain

$$\begin{aligned}
I_{SC} \frac{E_0}{E} &= (I_{SC0} + \alpha_{Isc} (T_C - T_0)) \\
&= \beta_0 + \beta_1 (T_C - T_0)
\end{aligned}
\tag{9}$$

Using measured  $I_{SC}$ ,  $E$  and  $T_C$ , a linear least-squares minimization (i.e., linear regression) obtains coefficients  $\beta_0$  and  $\beta_1$  from which  $\alpha_{Isc}$  is determined:

$$\alpha_{Isc} = \beta_1. \tag{10}$$

Figure 2 illustrates the determination of  $\alpha_{Isc}$ .

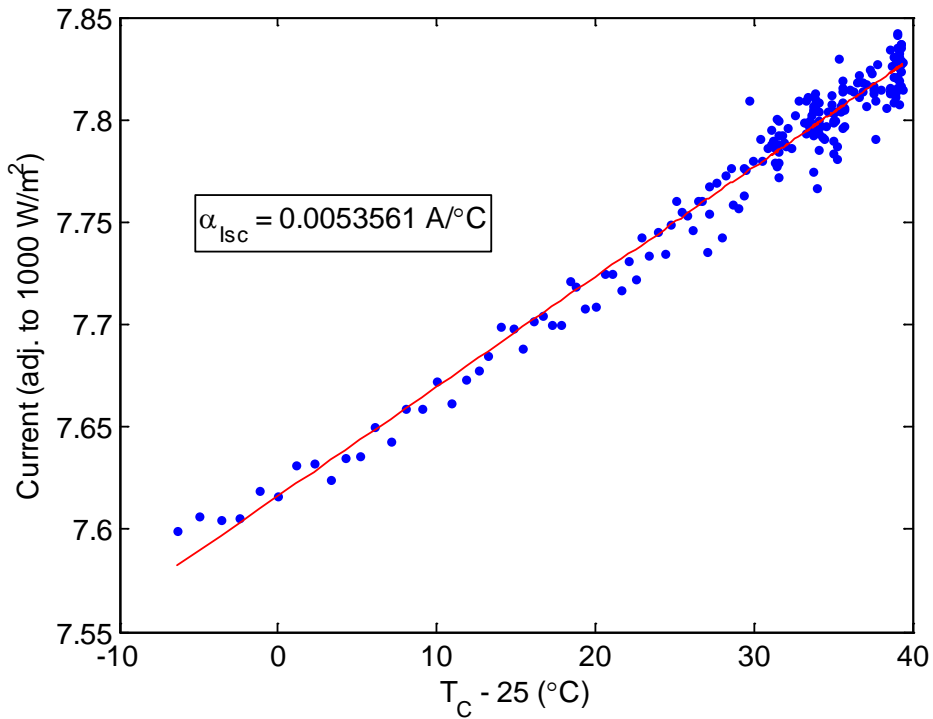


**Figure 2. Determination of  $\alpha_{Isc}$ .**

*Step 2: Determine diode factor terms.*

The method presented in [5] was illustrated by application to the single diode model in [10] in which the diode factor is constant and could be determined by a linear regression between  $V_{OC}$  and  $\ln(E/E_0)$ . For the PVsyst single diode model the parameters involved in the diode factor (i.e.,  $\gamma_0$  and  $\mu_\gamma$ ) are determined by first estimating  $\gamma$  for each IV curve from measured  $V_{OC}$ ,  $V_{OC}$  and  $I_{SC}$  but the technique requires a value for  $R_{SH}$  for each IV curve.

Step 2a: Estimate initial value for  $R_{SH}$ .

For each I-V curve, we determine an initial value for  $R_{SH}$  with a regression involving the co-content  $CC$ , i.e., an integral of the I-V curve over voltage. The co-content is stated in [11] to be exactly equal to a polynomial in  $V$  and  $I = I(V)$  (details are shown in [5], Appendix C):

$$CC(V) = \int_0^V (I_{SC} - I(v)) dv = c_1 V + c_2 (I_{SC} - I) + c_3 V (I_{SC} - I) + c_4 V^2 + c_5 (I_{SC} - I)^2 \quad (11)$$

Using Eq. (11) value for  $R_{SH}$  is determined as

$$R_{SH} = 1/2c_4 \quad ([11], \text{Eq. 11}) \quad (12)$$

where the constant  $c_4$  is obtained by regression. As presented in [5], the integral in Eq. (11) is evaluated using a quadratic spline that respects the decreasing, convex shape of the I-V curve, and the linear regression is performed after a principal components transformation to orthogonalize the predictors. Appendix C in [5] provides details behind the spline approximation and the principal components transformation. We note this this technique obtains reasonable values for most, but not all, measured I-V curves on which we have tested the methods. Figure 3 displays examples of I-V curves where the method fails; in most cases, the failure arises from increasing current with increasing voltage, indicating problems with the underlying measurements.

Step 2b: Estimate diode factor  $\gamma_0$  and temperature coefficient  $\mu_\gamma$ .

The parameters  $\gamma_0$  and  $\mu_\gamma$  are estimated by a linear regression:

$$\begin{aligned} \ln\left(I_{SC} - \frac{V_{OC}}{R_{SH}}\right) - 3 \ln\left(\frac{T_C}{T_0}\right) &= c_1 + c_2 \frac{q}{k} \left(\frac{1}{T_C} - \frac{1}{T_0}\right) - c_3 \frac{q}{k} \left(\frac{1}{T_C} - \frac{1}{T_0}\right) (T_C - T_0) \\ &+ c_4 \frac{V_{OC}}{V_{th}} - c_5 \frac{V_{OC}}{V_{th}} (T_C - T_0) \end{aligned} \quad (13)$$

where

$$\gamma_0 = \frac{1}{c_4} \quad (14)$$

$$\mu_\gamma = c_5 \gamma_0^2 \quad (15)$$

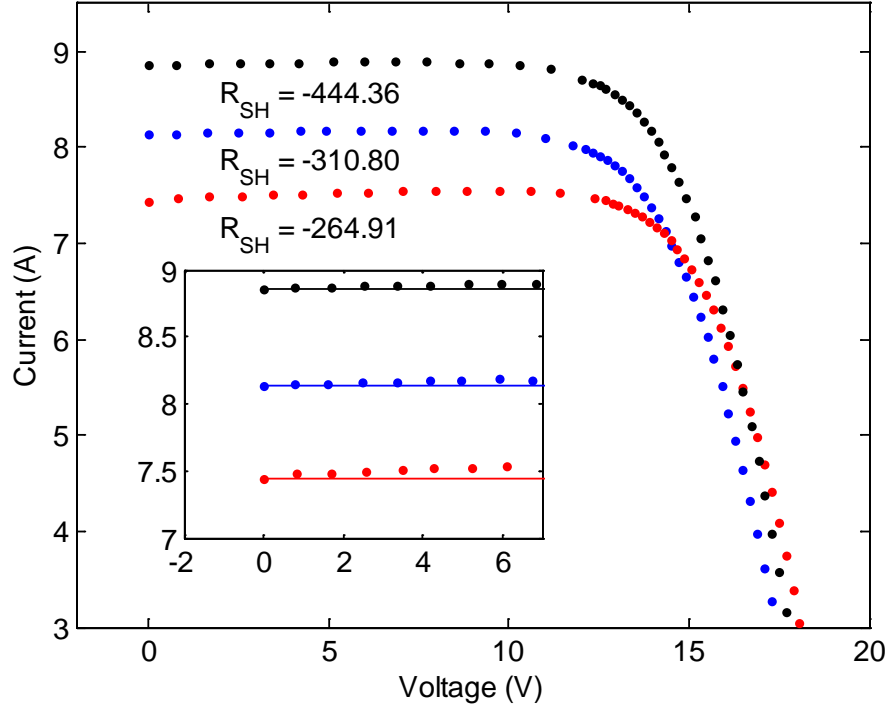


**Figure 3. Examples of measured I-V curves for which  $R_{SH} < 0$ .**

Eq. (13) results from combining Eq. (1) at  $I_{SC}$  and at  $V_{OC}$  with Eq. (3) along with several approximations described here. At  $I_{SC}$  from Eq. (1) we obtain

$$I_{SC} = I_L + I_o - I_o \exp\left(\frac{I_{SC}R_s}{\gamma V_{th}}\right) - \frac{I_{SC}R_s}{R_{SH}} \quad (16)$$

and from Eq. (1) at  $V_{OC}$

$$0 = I_L + I_o - I_o \exp\left(\frac{V_{OC}}{\gamma V_{th}}\right) - \frac{V_{OC}}{R_{SH}} \quad (17)$$

Subtracting Eq. (17) from Eq. (16)

$$\begin{aligned} I_{SC} &= I_o \exp\left(\frac{V_{OC}}{\gamma V_{th}}\right) - I_o \exp\left(\frac{I_{SC}R_s}{\gamma V_{th}}\right) + \frac{V_{OC} - I_{SC}R_s}{R_{SH}} \\ &\approx I_o \exp\left(\frac{V_{OC}}{\gamma V_{th}}\right) + \frac{V_{OC} - I_{SC}R_s}{R_{SH}} \end{aligned} \quad (18)$$

where the approximation is justified generally because  $I_{SC} < 10\text{A}$ ,  $R_S < 1\Omega$ ,  $\gamma V_{th} \approx 2\text{V}$ , and  $I_O < 10^{-7}$  thus  $I_O \exp(I_{SC} R_S / \gamma V_{th}) < 10^{-7} \exp(5) \approx 1.5 \times 10^{-5}$ . Solving Eq. (18) for  $I_{SC}$  and approximating  $\frac{R_{SH}}{R_{SH} + R_S} \approx 1$

$$\begin{aligned} I_{SC} &\approx \frac{R_{SH}}{R_{SH} + R_S} \left[ \frac{V_{OC}}{R_{SH}} + I_O \exp\left(\frac{V_{OC}}{\gamma V_{th}}\right) \right] \\ &\approx \frac{V_{OC}}{R_{SH}} + I_O \exp\left(\frac{V_{OC}}{\gamma V_{th}}\right) \end{aligned} \quad (19)$$

substituting Eq. (3) and applying a logarithm obtains

$$\ln\left(I_{SC} - \frac{V_{OC}}{R_{SH}}\right) \approx \ln I_{O0} + 3 \ln\left(\frac{T_C}{T_0}\right) + \frac{q\varepsilon_G}{k\gamma} \left(\frac{1}{T_0} - \frac{1}{T_C}\right) + \frac{V_{OC}}{\gamma V_{th}} \quad (20)$$

From Eq. (4) and the general assumption that  $\frac{\mu_\gamma}{\gamma_0}(T_C - T_0) \ll 1$  we approximate

$$\begin{aligned} \frac{1}{\gamma} &= \frac{1}{\gamma_0 + \mu_\gamma(T_C - T_0)} = \frac{1}{\gamma_0} \frac{1}{1 + \frac{\mu_\gamma}{\gamma_0}(T_C - T_0)} \\ &\approx \frac{1}{\gamma_0} \left(1 - \frac{\mu_\gamma}{\gamma_0}(T_C - T_0)\right) = \frac{1}{\gamma_0} - \frac{\mu_\gamma}{\gamma_0^2}(T_C - T_0) \end{aligned} \quad (21)$$

Substituting Eq. (21) into Eq. (20) and rearranging obtains

$$\begin{aligned} \ln\left(I_{SC} - \frac{V_{OC}}{R_{SH}}\right) - 3 \ln\left(\frac{T_C}{T_0}\right) &\approx \ln I_{O0} + \frac{\varepsilon_G}{\gamma_0} \frac{q}{k} \left(\frac{1}{T_0} - \frac{1}{T_C}\right) - \frac{\varepsilon_G \mu_\gamma}{\gamma_0^2} \frac{q}{k} \left(\frac{1}{T_0} - \frac{1}{T_C}\right) (T_C - T_0) \\ &\quad + \frac{1}{\gamma_0} \frac{V_{OC}}{V_{th}} - \frac{\mu_\gamma}{\gamma_0^2} \frac{V_{OC}}{V_{th}} (T_C - T_0) \end{aligned} \quad (22)$$

which is in the form of Eq. (13), with all terms on the left hand side known from measurements, and the unknown terms on the right hand side comprising  $\ln I_{O0}$ ,  $\varepsilon_G/\gamma_0$ ,  $\varepsilon_G \mu_\gamma/\gamma_0^2$ ,  $1/\gamma_0$  and  $\mu_\gamma/\gamma_0^2$ . We determine  $\gamma_0$  and  $\mu_\gamma$  as indicated in Eq. (14) and Eq. (15) because the predictors  $V_{OC}/V_{th}$  and  $V_{OC}/V_{th}(T_C - T_0)$  are generally an order of magnitude greater than the quantities  $q/k(1/T_0 - 1/T_C)$  and  $q/k(1/T_0 - 1/T_C)(T_C - T_0)$ , respectively. Figure 4 compares the regression model quantities (i.e.,  $V_{OC}/V_{th}$  and  $V_{OC}/V_{th}(T_C - T_0)$ ) from the I-V data and as calculated using the estimated values for  $\gamma_0$  and  $\mu_\gamma$ .

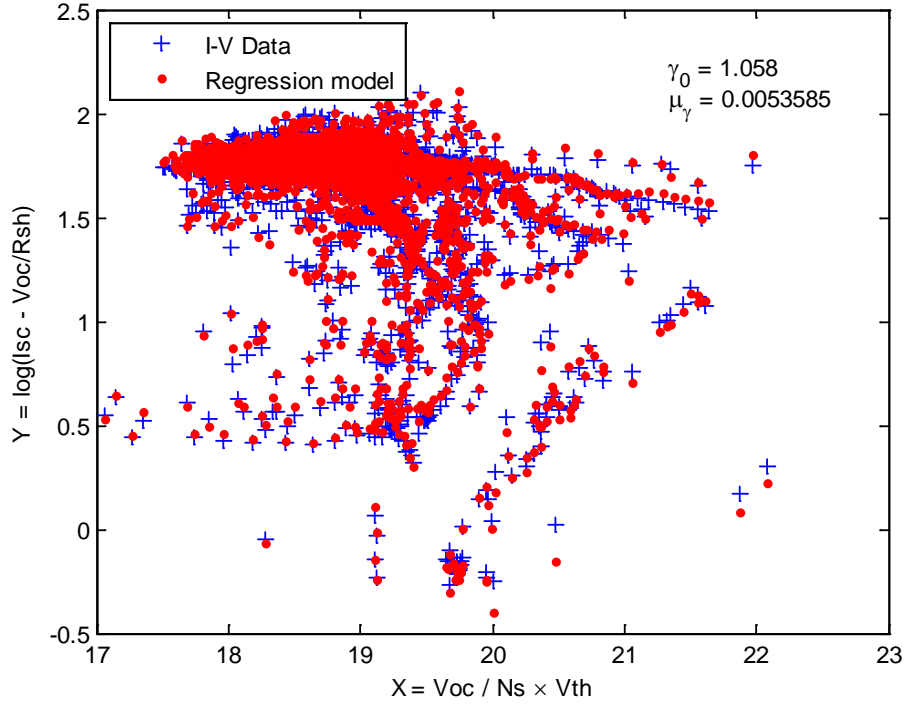


**Figure 4. Estimation of diode factor parameters.**

*Step 3: Determine parameters for each I-V curve*

With  $\gamma_0$  and  $\mu_\gamma$  determined, a value for the diode factor  $\gamma$  for each I-V curve can be computed using Eq. (4). Using  $\gamma$  the next step determines values for  $R_S$ ,  $I_O$ ,  $I_L$  and  $R_{SH}$  for each I-V curve.

Step 3a: Find initial values for  $R_S$ ,  $I_O$ ,  $I_L$ .

The initial estimate of  $I_O$  is obtained from Eq. (19):

$$I_O = \left( I_{SC} - \frac{V_{OC}}{R_{SH}} \right) \exp \left( -\frac{V_{OC}}{\gamma V_{th}} \right) \quad (23)$$

With a value for  $I_O$  in hand, the initial estimate of  $R_S$  is obtained from the slope of the I-V curve near  $V_{OC}$  (but not *at*  $V_{OC}$ ). Ideally, the derivative  $\frac{dI}{dV}$  will be negative and smoothly decreasing as  $V \rightarrow V_{OC}$ . Estimating the derivative from data requires use of some kind of numeric differentiation scheme. For measured I-V curves we cannot assume that the points comprising the I-V curve are taken at equally-spaced voltage values and consequently most common finite

difference approximations (e.g., [12]) are not suitable. We employ a fifth order finite difference technique (i.e., Eq. A5b in [13]) which accommodates unequally-spaced data to estimate

$$I'_V(V_k) = \left. \frac{dI}{dV} \right|_{V=V_k}, k=1, \dots, M \quad (24)$$

for data at voltages  $V_k$  where  $L = 0.5V_{OC} < V_k < 0.9V_{OC} = R$  and  $k=1, \dots, M$ . Then, we estimate  $R_S$  as the average (Eq. (25))

$$R_S \cong \frac{1}{M} \sum_{k=1}^M R_{S,k} \quad (25)$$

where

$$R_{S,k} = \frac{\gamma V_{th}}{I_{SC}} \left[ \ln \left( - (R_{SH} I'_V(V_k) + 1) \frac{\gamma V_{th}}{R_{SH} I_O} \right) - \frac{V_k}{\gamma V_{th}} \right] \quad (26)$$

for points where  $R_{SH} I'_V(V_k) + 1 < 0$ . Justification for Eq. (26) is provided in [5]. Lastly,  $I_L$  is estimated by evaluating Eq. (1) at  $I_{SC}$ :

$$I_L = I_{SC} - I_O + I_O \exp \left( \frac{R_S I_{SC}}{\gamma V_{th}} \right) + \frac{R_S I_{SC}}{R_{SH}} \quad (27)$$

### Step 3b: Filter out I-V curves with bad parameter sets.

Once initial estimates are obtained, the algorithm filters the parameter sets to exclude I-V curves where the parameter estimates indicate problems. An I-V curve is excluded if the corresponding parameter estimates meet any of the following criteria:

- The value for  $R_{SH}$  is negative (indicating that current may be increasing with increasing voltage) or is indeterminate (indicating a lack of data or a problem with the regression which determines the coefficient  $c_4$  in Eq. (12)).
- The value for  $R_S$  is negative, has a non-zero imaginary component, is indeterminate or is greater than  $R_{SH}$ .
- The value for  $I_O$  is zero, negative, or has a non-zero imaginary component.

In addition, the algorithm expects that the PV device is substantially linear, i.e., the measured short-circuit current  $I_{SC}$  is nearly proportional to effective irradiance  $E$  (or to broadband POA irradiance  $G_{POA}$ ). An empirical efficiency  $\eta$  is obtained by regressing  $I_{SC}$  onto  $E$ , i.e.,

$$I_{SC} = \eta \frac{E}{E_0} \quad (28)$$

and the residual  $\varepsilon = \eta(E/E_0) - I_{SC}$  is used to exclude I-V curves where  $|\varepsilon| > 0.05I_{SC}$  reasoning that these errors occur when there are substantial differences between  $E$  (or  $G_{POA}$ ) and  $I_{SC}$  due

to shading or other external factors. When these rules are applied to data obtained at SNL's laboratory typically only a few (<1%) I-V curves are filtered out, and these I-V curves usually display obvious problems such as increasing current as voltage increases.

Step 3c: Update initial estimates of  $R_{SH}$ ,  $R_S$ ,  $I_O$  and  $I_L$  to obtain final values for each I-V curve.

The initial estimates  $R_{SH}$ ,  $R_S$ ,  $I_O$  and  $I_L$  may result in poor matches to measured  $V_{OC}$ ,  $V_{MP}$  and  $I_{MP}$ . Parameters are updated in order as follows:

1.  $R_{SH}$  is adjusted to match  $V_{MP}$  by a fixed point iteration, using previous values for  $R_S$ ,  $I_O$  and  $I_L$ ;
2.  $R_S$  is updated to match  $V_{MP}$  calculated using the new value for  $R_{SH}$  and previous values for  $I_O$  and  $I_L$ ;
3.  $I_O$  is adjusted to match  $V_{OC}$  by a method similar to Newton's method using new values for  $R_{SH}$  and  $R_S$  and the previous value for  $I_L$ ;
4.  $I_L$  is updated to match  $I_{SC}$  by Eq. (27) using new values for  $R_{SH}$ ,  $R_S$  and  $I_O$ .

We solve for the updated value of  $R_{SH}$  by fixing  $I_O$  and  $I_L$  at their previous values and iterating the following which adjusted the calculated maximum power point towards the measurements:

$$R_{SH,k+1} = \frac{1+W(\psi)}{W(\psi)} \left[ \frac{I_L + I_O}{I_{MP}} R_{SH,k} - \frac{nV_{th}W(\psi)}{I_{MP}} - \frac{2V_{MP}}{I_{MP}} \right] \quad (29)$$

where  $W(x)$  is the Lambert's W function and

$$\psi = \frac{I_O R_{SH}}{nV_{th}} \exp\left(\frac{R_{SH}(I_L + I_O - I_{MP})}{nV_{th}}\right) \quad (30)$$

Convergence of Eq. (29) is slow and requires several hundred iterations in our testing. Justification for Eq. (29) is provided in [5]. The value for  $R_S$  is updated to be consistent with the new value for  $R_{SH}$  and the measured maximum power point:

$$R_S = \frac{I_L + I_O - I_{MP}}{I_{MP}} R_{SH} - \frac{nV_{th}}{I_{MP}} W(\psi) - \frac{V_{MP}}{I_{MP}} \quad (31)$$

Next,  $I_O$  is adjusted so that calculated  $V_{OC}$  matches measured  $V_{OC}$ . The updated value is found by iterating

$$I_{O,k+1} = I_{O,k} \times \left[ 1 + \frac{2(V_{OC}(I_{O,k}) - \hat{V}_{OC})}{2nV_{th} - (V_{OC}(I_{O,k}) - \hat{V}_{OC})} \right] \quad (32)$$

where we compute  $V_{OC}(I_{O,k})$  from

$$V_{OC} = (I_L + I_O)R_{SH} - nV_{th}W(\psi) \quad (33)$$

Convergence of Eq. (32) is rapid; in our testing ten iterations suffice. Lastly,  $I_L$  is updated to match measured  $I_{SC}$  using updated values for  $R_{SH}$ ,  $R_S$  and  $I_O$  in Eq. (27).

**Step 3d: Test for convergence.** The parameter estimates for an I-V curve are considered converged when the maximum difference between the predicted  $I_{MP}$ ,  $V_{MP}$  and  $P_{MP}$  and the corresponding measurements are all less than 0.002% of the measured values. We also fix an (arbitrary) upper limit on the number of iterations (e.g., 10). The threshold for precision and the iteration limit can be easily changed. Figure 5 shows the differences between each I-V curve's performance points (maximum power, short circuit and open circuit) and the points on the corresponding fitted IV curve for our example module data. The small magnitude of the errors indicates that the algorithm is well-converged through Step 3c.

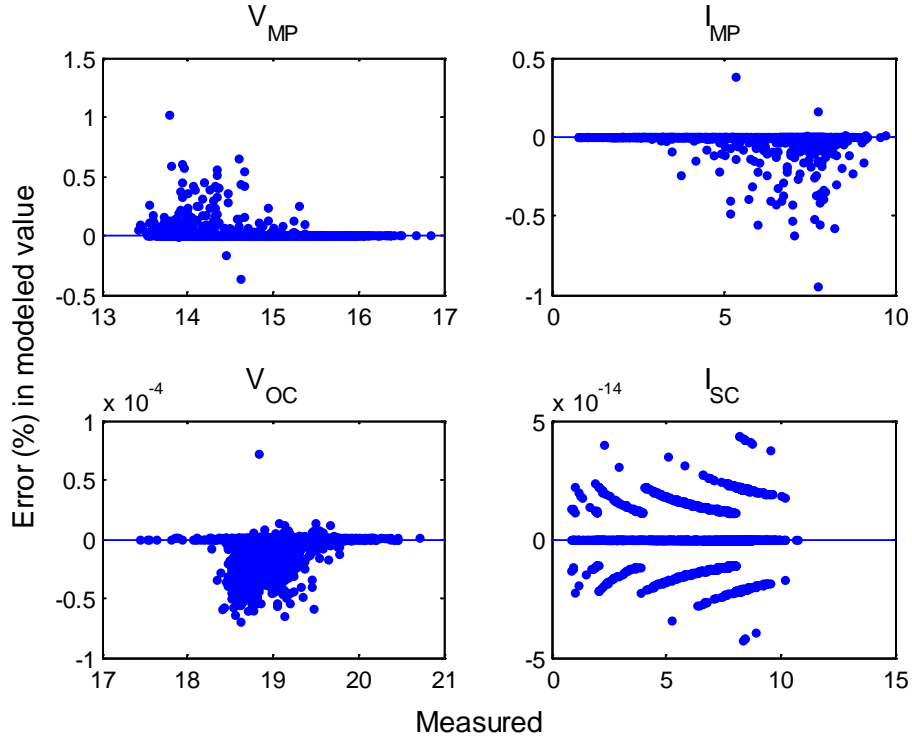


**Figure 5. Error (percent) in performance parameters for fitted I-V curves.**

*Step 4: Obtain parameter values for the PVsyst single diode model*

Here, we determine values for  $I_{L0}$ ,  $I_{O0}$ ,  $\varepsilon_G$ ,  $\gamma_0$ ,  $\mu_\gamma$ ,  $R_{SH,0}$ ,  $R_{SH,ref}$ ,  $R_{SH,exp}$  and  $R_{S0}$  from the set of five parameter values determined for each I-V curve.

A value for  $I_{L0}$  is found by rearranging Eq. (2) as

$$I_{L0} = I_L \frac{E_0}{E} - \alpha_{Isc} (T_C - T_0) \quad (34)$$

and estimate  $I_{L0}$  as the average value of the right hand side of Eq. (34) over all I-V curves. Figure 6 illustrates the resulting value of  $I_{L0}$ . The values for  $I_L$  which are extracted from each I-V curve are compared with the values predicted by Eq. (2) where  $I_{L0}$  is estimated by Eq. (34) and  $\alpha_{Isc} = 0.0046 \text{ A/}^\circ\text{C}$ .

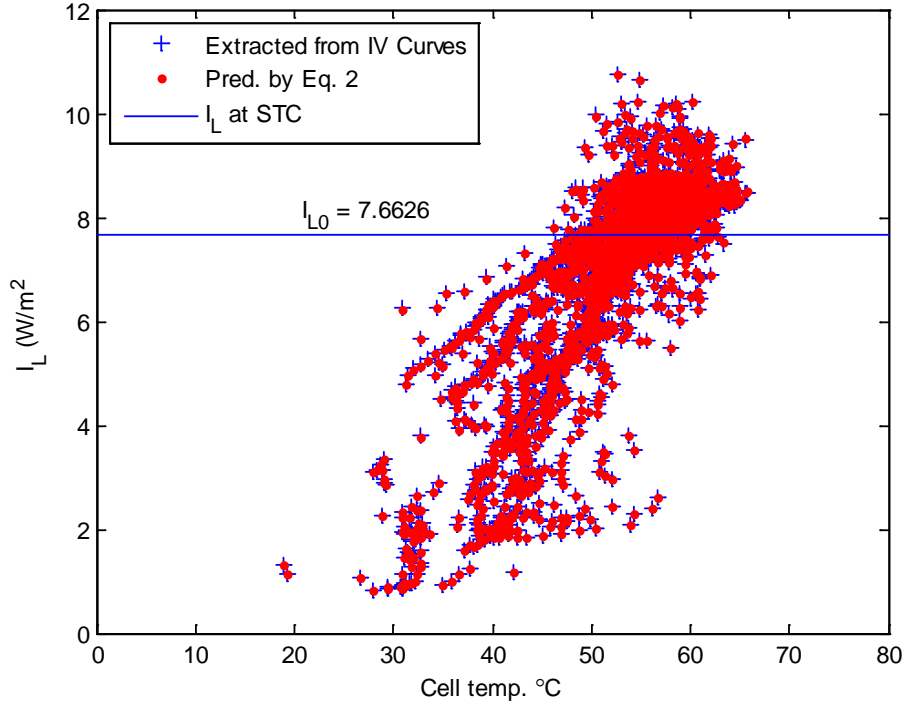


**Figure 6. Determination of  $I_{L0}$ .**

We estimate  $I_{o0}$  and  $\varepsilon_G$  from Eq. (3) by re-arranging as

$$\ln(I_o) - 3 \ln\left(\frac{T_C}{T_0}\right) = \ln I_{o0} + \frac{q}{k\gamma} \left(\frac{1}{T_0} - \frac{1}{T_C}\right) \varepsilon_G \quad (35)$$

and by regressing  $\ln(I_o) - 3 \ln\left(\frac{T_C}{T_0}\right)$  onto  $\frac{q}{k\gamma} \left(\frac{1}{T_0} - \frac{1}{T_C}\right)$ . We observed during testing that imposing a theoretical value for  $\varepsilon_G$  in Eq. (35) often results in significant disagreement between values of  $I_o$  calculated by Eq. (3) and values determined for each I-V curve in Step 3. Figure 7 compares the values of  $I_o$  that are extracted from each I-V curve to the values predicted from Eq. (3) using the estimated value of  $I_{o0}$  and  $\varepsilon_G$ .

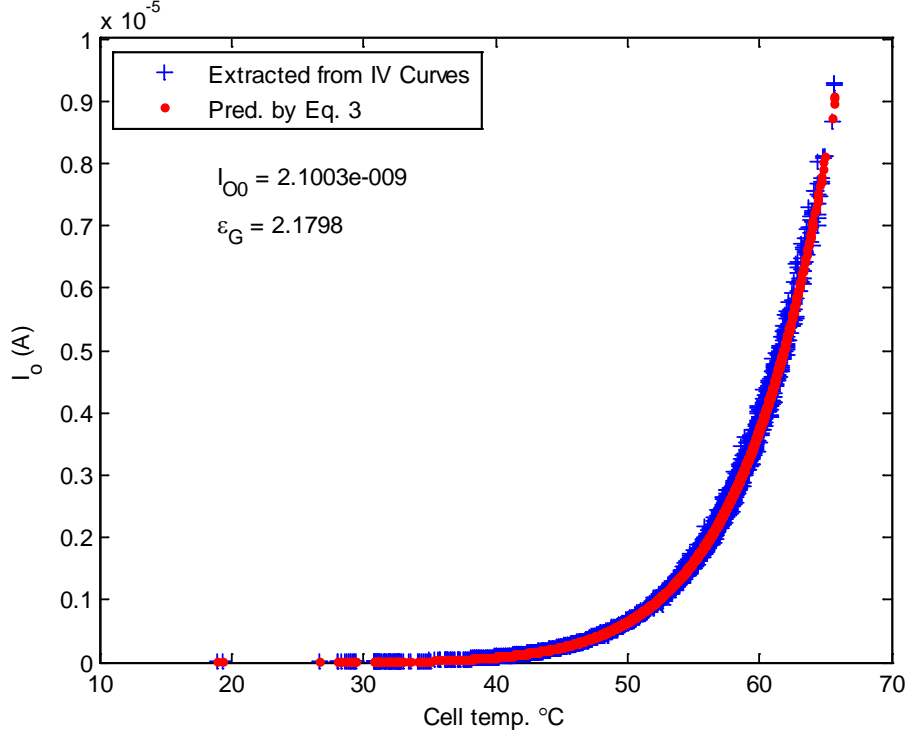


**Figure 7. Determination of  $I_{00}$  and  $\epsilon_G$ .**

Values for  $R_{SH,0}$ ,  $R_{SH,ref}$  and  $R_{SH,exp}$  are determined by nonlinear minimization. The equations relating  $R_{SH}$  to effective irradiance  $E$  (Eq. (36) and Eq. (37)) are defined piecewise and are nonlinear, and we found no means to obtain these parameters from approximations or through transformations that would formulate a minimization problem having a closed-form solution (e.g., least-squares).

$$R_{SH} = R_{SH,base} + (R_{SH,0} - R_{SH,base}) \exp\left(-R_{SH,exp} \frac{E}{E_0}\right) \quad (36)$$

$$R_{SH,base} = \max\left[\frac{R_{SH,ref} - R_{SH,0} \exp(-R_{sh,exp})}{1 - \exp(-R_{sh,exp})}, 0\right] \quad (37)$$

Moreover, we found that the values for  $R_{SH}$  estimated in Step 3 can vary over several orders of magnitude for I-V curves with similar effective irradiance, and that this variation appears to result primarily from relatively minor variations in the current measurements. Consequently when determined jointly the optimum values for  $R_{SH,0}$ ,  $R_{SH,ref}$  and  $R_{SH,exp}$  are quite sensitive to minor variations in the data. For this reason, we elected to fix  $R_{SH,exp} = 5.5$ , i.e., at the PVsyst default value, because the parameters  $R_{SH,0}$  and  $R_{SH,ref}$  appear to be less sensitive to large variation in the values for  $R_{SH}$ , and also to use a logarithm to reduce the influence of extreme values for  $R_{SH}$ . We determine  $R_{SH,0}$  and  $R_{SH,ref}$  jointly by minimizing

$$C(R_{SH}(R_{SH,ref}, R_{SH,0})) = \sum (\log_{10} R_{SH}(R_{SH,ref}, R_{SH,0}) - \log_{10} R_{SH})^2 \quad (38)$$

where  $R_{SH}(R_{SH,ref}, R_{SH,0})$  is computed as indicated in Eq. (36) and Eq. (37) with  $R_{SH,exp} = 5.5$ ,  $R_{SH}$  is the value determined for a measured I-V curve and the summation is over all measured I-V curves. A number of methods can be applied to minimize Eq. (38). We used a gradient descent technique that requires an initial estimate of  $R_{SH,0}$  and  $R_{SH,ref}$ . The initial value of  $R_{SH,0}$  is set as the average of  $R_{SH}$  for effective irradiance  $< 400 \text{ W/m}^2$ , and the initial value for  $R_{SH,ref}$  is the average of  $R_{SH,ref}$  for effective irradiance  $> 400 \text{ W/m}^2$ . Figure 8 compares values of  $R_{SH}$  extracted from each measured I-V curve with values predicted by Eq. (5) using the determined values for  $R_{SH,0}$ ,  $R_{SH,ref}$  and  $R_{SH,exp}$ .

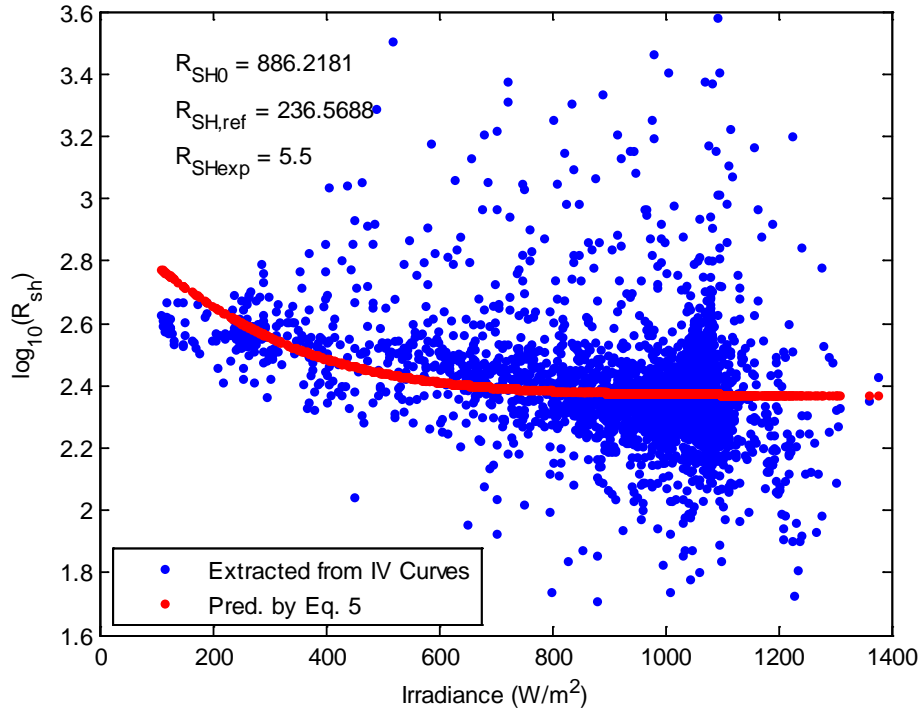


**Figure 8. Determination of parameters for  $R_{SH}$ .**

Finally, we estimate  $R_{S0}$  as the average of the values for  $R_S$  determined for each I-V curve with effective irradiance  $> 400 \text{ W/m}^2$ . Figure 9 compares the values of  $R_S$  with the estimated value for  $R_{S0}$ .

Table 1 summarizes model parameters determined for the example module, and module performance parameters predicted by the model.

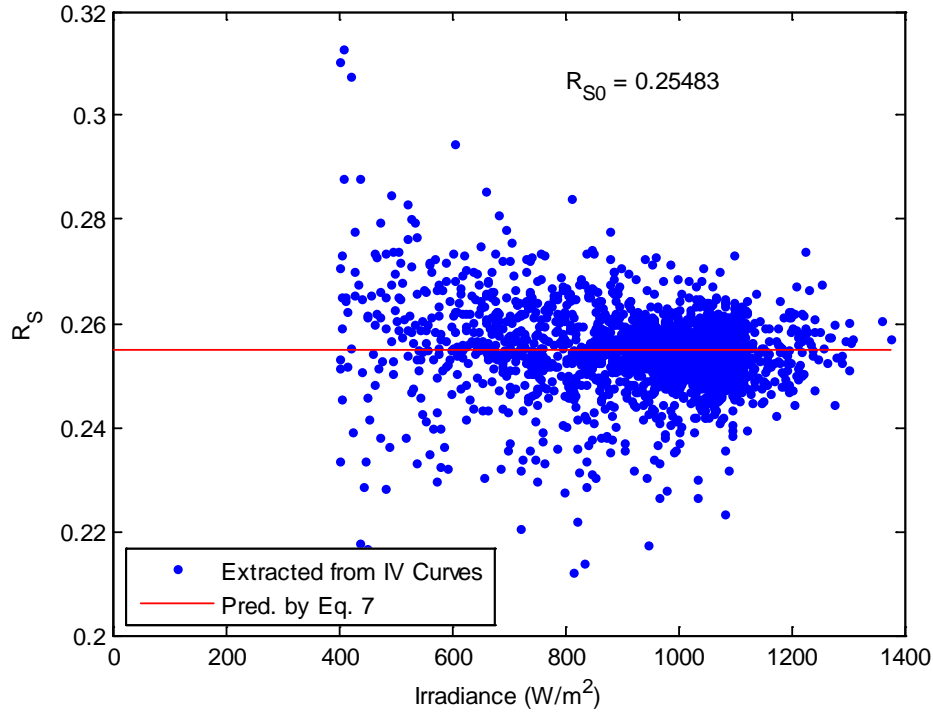


**Figure 9. Determination of  $R_{S0}$ .**

**Table 1. Parameters for example module.**

Model Parameter	Value	Model Parameter	Value
$\alpha_{Isc}$ (A/°C) <sup>1</sup>	0.0054	$I_{SC0}$ (A)	7.654
$I_{L0}$ (A)	7.663	$V_{OC0}$ (V)	21.53
$I_{O0}$ (nA)	2.100	$I_{MP0}$ (A)	7.127
$\varepsilon_G$ (eV)	2.180	$V_{MP0}$ (V)	16.97
$R_{S0}$ (Ω)	0.2548	$P_{MP0}$ (W)	120.9
$R_{SH0}$ (Ω)	886.2	$FF$ (unitless)	0.7337
$R_{SH,ref}$ (Ω)	236.6	$\gamma_{Pmp}$ (W/°C) <sup>2</sup>	-0.6746
$R_{SH,exp}$	5.5	$\alpha_{Imp}$ (A/°C) <sup>2</sup>	-0.0022
$\gamma_0$ (unitless)	1.058	$\beta_{Voc}$ (V/°C) <sup>2</sup>	-0.0819
$\mu_\gamma$ (1/°C)	0.0054	$\beta_{Vmp}$ (V/°C) <sup>2</sup>	-0.0894

<sup>1</sup> determined as described in Section 3.2, Step 1

<sup>2</sup> computed from simulated I-V curves with effective irradiance set equal to 1000 W/m<sup>2</sup>; see [14] for method details.

### 3. QUALITATIVE COMPARISON WITH OTHER METHODS

Other methods are available for estimating parameters for single diode models (see discussion in [5].) However, for PVsyst™ version 6 specifically, there are two other methods available. PVsyst™ version 6 includes a capability to estimate model parameters from data loaded into the software. In earlier versions, significant prediction errors were observed when using parameters determined using the built-in estimation tools [6]. The capability in PVsyst™ version 6 is improved over earlier versions of the software [7], but we have not carried out an assessment of model prediction accuracy when using parameter estimated by the PVsyst™ version 6 tools.

To overcome these shortcomings, Sauer et al. [6], [7] developed an alternative method to determine all parameters for PVsyst™ version 6 using a three-step procedure. The method requires the capability to measure I-V curves with either temperature or irradiance held constant and thus is applicable primarily when using suitable indoor test apparatus. First, temperature coefficients are determined by separate testing and the parameter  $\varepsilon_G$  is set to a value taken from literature for the module's cell material. Second, measured I-V curves at fixed temperature (i.e., 25°C) are fit in an optimization approach to obtain values for the parameters  $I_{L0}$ ,  $I_{O0}$ ,  $\gamma_0$ ,  $R_{SH,0}$ ,  $R_{SH,ref}$ ,  $R_{SHexp}$  and  $R_{S0}$  [6]. Third, a value for  $\mu_\gamma$  is determined using I-V curves at different temperatures in conjunction with the already-determined values for  $I_{L0}$ ,  $I_{O0}$ ,  $\gamma_0$ ,  $R_{SH,0}$ ,  $R_{SH,ref}$ ,  $R_{SHexp}$  and  $R_{S0}$ .

By contrast, our method can operate on data collected either outdoors or indoors. Similar to [6] we first determine temperature coefficients by separate testing. We next determine  $\gamma_0$  and  $\mu_\gamma$  using the full set of I-V curves, i.e., with co-varying temperature and irradiance, then use these parameters to determine a vector of values  $I_L$ ,  $I_O$ ,  $R_{SH}$  and  $R_S$  for each I-V curve. Regression between  $I_L$ ,  $I_O$ ,  $R_{SH}$  and  $R_S$ , and temperature and irradiance then obtains values for values for  $I_{L0}$ ,  $I_{O0}$ ,  $\varepsilon_G$ ,  $R_{SH,0}$ ,  $R_{SH,ref}$ ,  $R_{SHexp}$  and  $R_{S0}$ . In particular we view  $\varepsilon_G$  as an empirical parameter whose value is set to best match the values of  $I_O$  for each I-V curve. Our values for  $\varepsilon_G$  depart substantially from the theoretical values, the imposition of which tends to significantly degrade the accuracy of the fitted model [5].

The methods in [6], [7] are structured to minimize the sum of differences between modeled and measured module efficiency at the maximum power point of each I-V curve. These methods will result in a model with relative predictive error (i.e., percent error) that is roughly equal at different irradiance and temperature conditions.

Our methods make no attempt to minimize error in predicting module efficiency, nor specifically to minimize prediction error across the range of irradiance and temperature conditions (beyond the minimization inherent in the regressions we perform). Because our methods seek to determine values for  $I_L$ ,  $I_O$ ,  $R_{SH}$  and  $R_S$  for each I-V curve, our methods are capable of exposing deficiencies in the equations used in PVsyst™ version 6 to describe how these quantities vary with temperature and irradiance, i.e., the auxiliary equations, Eq. (2) through Eq. (7).

In our view the methods in [6], [7] may be preferred when the objective is to empirically determine parameter sets that minimize overall prediction error of the model encoded in PVsyst<sup>TM</sup> version 6. In contrast, our methods offer the potential to indicate how to vary the equations of the PVsyst<sup>TM</sup> version 6 model in order to better match the measured module performance.

## 4. REFERENCES

1. University of Geneva, *User's Guide PVsyst Contextual Help*, <http://files.pvsyst.com/pvsyst5.pdf>, Accessed.
2. Mermoud, A. and T. Lejeune. *Performance Assessment Of A Simulation Model For Pv Modules Of Any Available Technology*. in *25th European Photovoltaic Solar Energy Conference*, 2010. Valencia, Spain.
3. Gray, J.L., *The Physics of the Solar Cell*, in *Handbook of Photovoltaic Science and Engineering*, A. Luque, Hegedus, S., Editor. 2011, John Wiley and Sons.
4. IEC, *IEC 61853-1 Ed. 1.0: Photovoltaic (PV) module performance testing and energy rating - Part I: Irradiance and temperature performance measurements and power rating*, 2011, International Electrotechnical Commission: Geneva, Switzerland.
5. Hansen, C., *Parameter Estimation for Single Diode Models of Photovoltaic Modules*, SAND2015-2065, Sandia National Laboratories, Albuquerque, NM, 2015.
6. Sauer, K.J. and T. Roessler, *Systematic Approaches to Ensure Correct Representation of Measured Multi-Irradiance Module Performance in PV System Energy Production Forecasting Software Programs*. *Photovoltaics, IEEE Journal of*, 2013. **3**(1): p. 422-428.
7. Sauer, K.J., T. Roessler, and C.W. Hansen, *Modeling the Irradiance and Temperature Dependence of Photovoltaic Modules in PVsyst*. *Photovoltaics, IEEE Journal of*, 2015. **5**(1): p. 152-158.
8. Dunn, L., M. Gostein, and K. Emery. *Comparison of Pyranometers vs. PV Reference Cells for Evaluation of PV Array Performance*. in *38th IEEE Photovoltaic Specialists Conference*, 2012. Austin, TX: IEEE.
9. Hansen, C., K.A. Klise, and J.S. Stein. *Data Requirements for Calibration of Photovoltaic System Models Using Monitored System Data*. in *42nd IEEE Photovoltaic Specialist Conference*, 2015. New Orleans, LA.
10. De Soto, W., S.A. Klein, and W.A. Beckman, *Improvement and validation of a model for photovoltaic array performance*. *Solar Energy*, 2006. **80**(1): p. 78-88.
11. Ortiz-Conde, A., F.J. García Sánchez, and J. Muci, *New method to extract the model parameters of solar cells from the explicit analytic solutions of their illuminated I–V characteristics*. *Solar Energy Materials and Solar Cells*, 2006. **90**(3): p. 352-361.
12. Burden, R.L. and J.D. Faires, *Numerical analysis*. 4th ed. The Prindle, Weber, and Schmidt series in mathematics. 1989, Boston: PWS-KENT Pub. Co. xv, 729 p.
13. Bowen, M.K. and R. Smith, *Derivative formulae and errors for non-uniformly spaced points*. *Proceedings of the Royal Society A: Mathematical, Physical and Engineering Science*, 2005. **461**(2059): p. 1975-1997.
14. Hansen, C., D. Riley, and M. Jaramillo. *Calibration of the Sandia Array Performance Model Using Indoor Measurements* in *IEEE Photovoltaic Specialists Conference*, 2012. Austin, TX.

## DISTRIBUTION

1 MS0899 Technical Library 9536 (electronic copy)





**Sandia National Laboratories**